

# $3 \times 10^8$ D-D Neutron Generation by High-Intensity Laser Irradiation onto the Inner Surface of Spherical CD Shells<sup>\*</sup>

Nakahiro SATOH, Takeshi WATARI, Katsunobu NISHIHARA, Koji MATSUKADO, Ryo YOSHIMURA, Naoki AKIYAMA, Masaru TAKAGI, Toshiyuki KAWASHIMA, Yuki ABE<sup>1)</sup>, Yasunobu ARIKAWA<sup>1)</sup>, Atsushi SUNAHARA<sup>2)</sup>, Yoichiro HIRONAKA<sup>1)</sup>, Keisuke SHIGEMORI<sup>1)</sup>, Shinsuke FUJIOKA<sup>1)</sup>, Mitsuo NAKAI<sup>1)</sup> and Hiroshi AZECHI<sup>1)</sup>

*Industries Development Laboratory, Central Research Laboratory, HAMAMATSU PHOTONICS K.K., 1820 Kurematsu-cho, Nishi-ku, Hamamatsu, Shizuoka 431-1202, Japan*

<sup>1)</sup>*Institute of Laser Engineering, Osaka University, 2-6 Yamadaoka, Suita, Osaka 565-0871, Japan*

<sup>2)</sup>*Institute of Laser Technology, 2-6 Yamadaoka, Suita, Osaka 565-0871, Japan*

(Received 1 June 2017 / Accepted 30 January 2018)

$3 \times 10^8$  deuterium-deuterium (D-D) neutron generation per pulse was achieved with one-sided laser irradiation through an inlet hole of a deuterated polystyrene shell and a laser intensity of  $(2-3) \times 10^{16}$  W/cm<sup>2</sup>. X-ray pinhole camera images displayed a surprisingly uniform hot core formation at the center of the shell. Neutron time-of-flight spectra were recorded at three different angles from the laser incident axis to investigate the directional dependence. The dependence of neutron yield on laser energy, shell diameter, and inlet hole diameter is also discussed. To explain the number of the observed neutrons, a simple model, based on a central expansion of two-electron-temperature (hot and cold) plasma, is presented under assumed hot and cold electron temperature. According to this model, more than  $10^{10}$  neutrons per pulse, the average amount required for many industrial applications, could be generated by using a higher intensity laser.

© 2018 The Japan Society of Plasma Science and Nuclear Fusion Research

Keywords: laser-driven neutron source, spherical shell, inner surface irradiation, two-electron-temperature plasma, neutron time-of-flight, hot core plasma, one-sided laser irradiation

DOI: 10.1585/pfr.13.2401028

## 1. Introduction

Laser-produced neutrons are expected to use in many industrial and medical applications, as their sources are mono-energetic, pulsed point neutron sources [1]. In addition to the implosion method by using high-energy lasers [2–4], there are other two main methods to obtain laser-driven neutron sources by using high-intensity laser. Ditmire *et al.* achieved repetitive neutron generation with the Coulomb explosion of atomic clusters of deuterium using a tabletop laser system with a laser intensity higher than  $10^{16}$  W/cm<sup>2</sup> [5–7]. Subsequently, we observed the repetitive generation of  $10^5$  neutrons via irradiation with a diode-pumped solid-state laser of intensity  $10^{18}$  W/cm<sup>2</sup> the spray of sub-micron particles of deuterated polystyrene (CD) [8]. Roth *et al.* reported, for a laser intensity of  $10^{20}$  W/cm<sup>2</sup>, a neutron emission flux of  $10^{10}$  n/sr from the interaction between lithium atoms and accelerated deuterium ions with energies up to 170 MeV produced by the laser break-out afterburner (BOA) mechanism [9].

Recently, we have been focusing on the use of lasers with moderate laser intensities of  $10^{16-17}$  W/cm<sup>2</sup> and a

pulse duration of about 100 ps. In this study, we chose an inner surface irradiation scheme through an inlet hole of a CD shell, to be suitable for such laser parameters. Daido *et al.* observed a neutron generation of up to  $10^8$  from the irradiation of the inner surface of a CD shell with six beams of GEKKO-XII (GXII), with an energy of 8.4 kJ and a pulse duration of 1000 ps [10]. In this study, we report the generation of  $3 \times 10^8$  neutrons per pulse achieved using the one-sided beam bundle of the GXII High-Intensity Plasma Experimental Research (GXII-HIPER) at the Institute of Laser Engineering (ILE, Osaka University), with a lower laser energy (2.2 - 2.6 kJ), a shorter pulse duration (100 ps), and an f-number of 3.01 [11]. We placed some neutron time-of-flight (nTOF) detectors at three different angles to understand the effects of the irradiation geometry on the neutron generation and determine the directional dependence.

In Sec. 2, we discuss the experimental results of the hot core formation, the neutron yield, the deuterium ion temperature, and the nTOF spectra observed at three different angles. In Sec. 3, we also present a simple model to explain the number of neutrons observed with scaling laws of neutron generation.

author's e-mail: naka@crl.hpk.co.jp

<sup>\*</sup>) This article is based on the presentation at the Conference on Laser Energy Science / Laser and Accelerator Neutron Sources and Applications 2017.

## 2. Experimental Results

We fabricated CD shells with various diameters with the conventional micro-encapsulation method [12] and made a laser inlet hole on the shell wall by laser machining, as shown in Fig. 1. The shell diameter ( $D_s$ ) varied between 0.5 and 2.0 mm. There were two types of inlet hole diameters ( $D_h$ ), one fixed at 0.5 mm, and the other variable, being half of the  $D_s$ . The laser intensity of the GXII-HIPER system was  $(2-3) \times 10^{16}$  W/cm<sup>2</sup>, a wavelength of 1.053  $\mu$ m, and a focal spot diameter of 300  $\mu$ m. Figure 2 illustrates a layout of the laser beam and of the detection system, which comprised an x-ray pinhole camera (XPC, wavelength range from 0.1 to 5 keV), placed at 90° with respect to the laser incident axis and five nTOF detectors arranged at the different angles. Three of five nTOF detectors were used to investigate the directional dependence.

Figure 3 depicts the XPC images in side view of the irradiated shell. The pixel size and the x-ray brightness were the same for all images. Surprisingly uniform hot cores were formed in the CD shell, even with the one-sided laser irradiation. Although the physical mechanisms of uniform hot core formation is still not well understood, both the multi-scattering of laser light within the cavity [13] and the heat conduction of high-energy electrons along the inner surface of the shell wall could be responsible for a rather

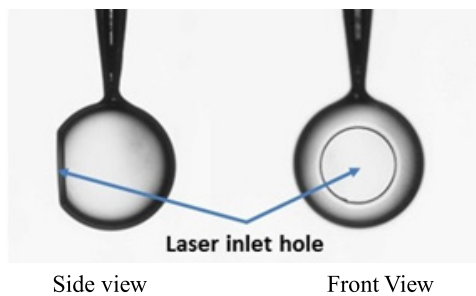


Fig. 1 CD spherical shell with a laser inlet hole. The  $D_s$  and  $D_h$  ranges are 0.5 - 2.0 mm and 0.25 - 1.0 mm, respectively.

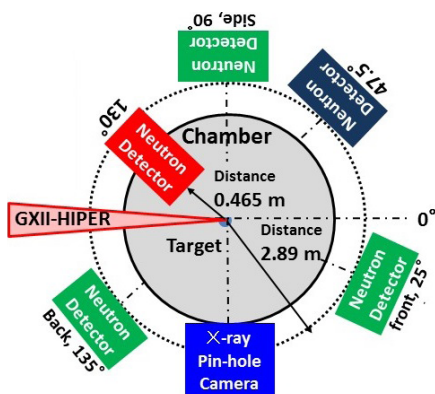


Fig. 2 Experimental setup: GXII-HIPER system, an XPC, and five nTOF detectors.

uniform ablation of the inner surface expanding toward the shell center.

Figure 4 depicts the neutron yields measured by the nTOF detector at 130° with respect to the laser incident axis and at a distance of 0.465 m, for various  $D_s$ . Blue triangles represent the data measured with the average laser energy of 2.55 kJ and the fixed  $D_h$  of 0.5 mm. The red squares correspond to the data with an average laser energy of 2.20 kJ and  $D_h$  being half of the  $D_s$ . By comparing the results from the average of laser energies of 2.55 and 2.20 kJ, it was observed that the increase in the number of neutrons generated was higher than the increase in the laser energy. The maximum neutron yield ( $3.1 \times 10^8$ ) was obtained with a laser energy of 2.47 kJ and a  $D_s$  of 1.89 mm. By comparing the results of 1 and 2 mm diameters, we can observe that the number of neutrons slightly increased with the increase of  $D_s$  when using the laser energy of 2.55 kJ and the fixed  $D_h$ , while it slightly decreased with the laser energy of 2.20 kJ. This difference might be attributed to the difference in the  $D_h/D_s$  ratio, in addition to the different laser energies. The loss of both the laser energy and the high-energy deuterium ions from the hole might be rel-

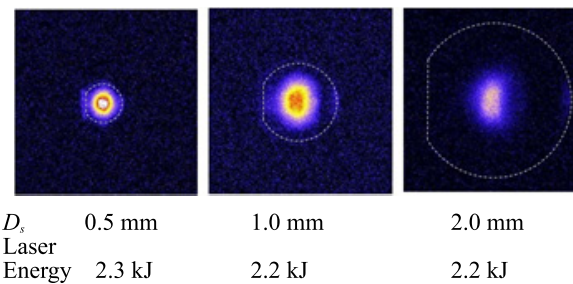


Fig. 3 XPC images. The shapes of the shells in side view are indicated by white dotted line in the images.

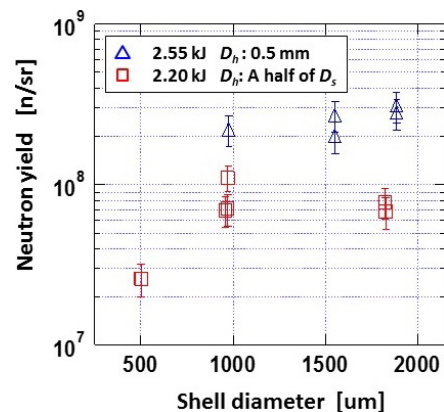


Fig. 4 Neutron yields for various  $D_s$ . The blue triangles represent the data obtained with average laser energy of 2.55 kJ and the  $D_h$  fixed at 0.5 mm for all the  $D_s$ , while the red squares correspond to an average laser energy of 2.20 kJ and a variable  $D_h$ .

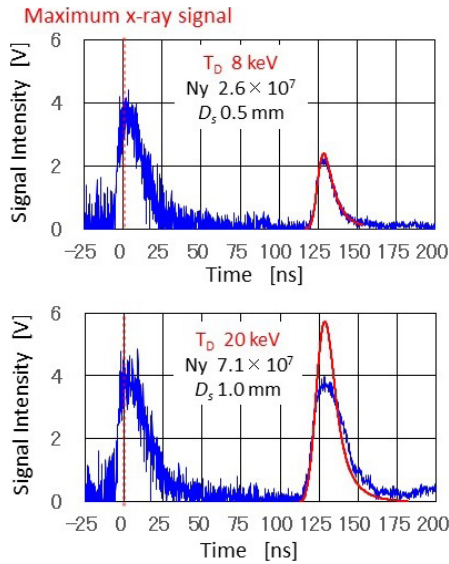


Fig. 5 nTOF spectra for the 0.5 mm  $D_s$  with neutron yield  $2.6 \times 10^7$  (above) and for the 1.0 mm  $D_s$  with neutron yield  $7.1 \times 10^7$  (bottom). The red dotted lines indicate the time of the maximum x-ray signal. The red solid lines represent the fitting curves obtained considering a thermo-nuclear fusion reaction of deuterium at an ion temperature of by 8 keV (above) and 20 keV (below).

atively large in the latter case, as  $D_h$  increased respect to  $D_s$ . The lower neutron yield was observed in the case of the 0.5 mm  $D_s$ , where the  $D_h$  of 0.25 mm was smaller than the focal spot diameter of 0.3 mm. Another study [13] reported a lower neutron yield for the same  $D_s$  of 0.5 mm. In that case, the laser could have not been well absorbed as the  $D_h$  of the open-tip gold cone used with CD shells was only 0.15 mm and, hence, much smaller than the focal spot diameter.

Figure 5 depicts the nTOF spectra (blue line), recorded by the detector placed at  $47.5^\circ$  with respect to the laser incident axis and at a distance of 2.89 m, for the 0.5 mm  $D_s$  with a neutron yield of  $2.6 \times 10^7$  (above) and for the 1.0 mm  $D_s$  with a neutron yield of  $7.1 \times 10^7$  (below). With a delay of 133 ns from the maximum x-ray signal (red dotted line), 2.45 MeV D-D neutron signals were detected. The red solid lines represent the fitting curves obtained by assuming a thermo-nuclear fusion reaction of the deuterium ions with a Maxwell energy distribution. For the above case, the neutron signal obtained for a deuterium ion temperature of 8 keV fits fairly well to the nTOF spectrum. In the bottom case, the nTOF signal was saturated and only the spectrum at the rising edge of the nTOF signal was used for the fitting, suggesting an ion temperature of 20 keV. However, such value of ion temperature might be too high to explain the observed neutron yield of  $7.1 \times 10^7$ .

Figure 6 depicts three nTOF spectra detected at the same distance of 2.89 m but different angles from the laser incident axis:  $25^\circ$  (front, red line),  $90^\circ$  (side, green line),

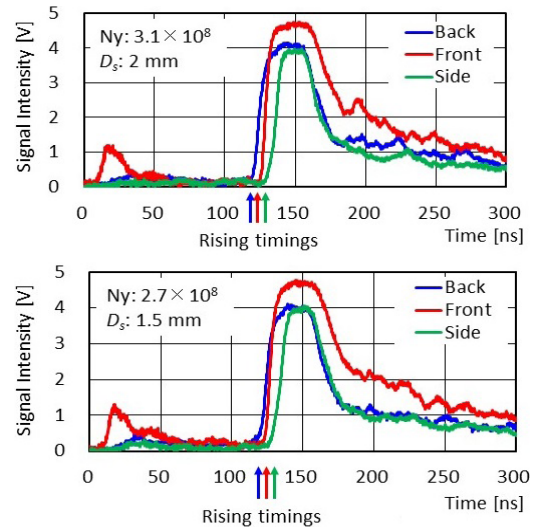


Fig. 6 nTOF spectra detected at the different angles:  $135^\circ$  (blue line),  $25^\circ$  (red line) and  $90^\circ$  (green line).

and  $135^\circ$  (back, blue line). The figures illustrate the results, for both a  $D_s$  of about 2.0 mm with a neutron yield of  $3.1 \times 10^8$  (above) and a  $D_s$  of about 1.5 mm with a neutron yield of  $2.7 \times 10^8$  (below). Blue, red, and green lines correspond to the data measured by the nTOF detectors placed, as shown in Fig. 2, respectively. The difference in the rising time of the nTOF signals among the three detectors spectra are clearly demonstrated. In both cases (above and below spectra), the fastest neutrons were observed by the back detector and the latest by the side one. This directional influence on the rising time suggests a strong anisotropy in the deuterium ion energy distribution. The shift from the 133 ns in the rising time observed by the back, front, and side detectors correspond to deuterium ion energies of  $\sim 900$  keV,  $\sim 500$  keV, and  $\sim 300$  keV, respectively. The ions with the highest energy were ejected from the area directly heated by the incident laser light and gave their momentum to the neutrons emitted toward the back detector, so that they were the fast ones to be detected. The ions ejected from the plasma heated by the reflected laser light and gave their momentum to the neutrons emitted toward the front detector might be fewer than those relied from the area directly heated by the incident laser.

### 3. Modeling and Scaling

It is well known that hot electrons coexist with cold electrons in laser-produced plasmas when  $I\lambda^2 > 10^{14}$  ( $\text{W}/\text{cm}^2 \cdot (\mu\text{m}^2)$ ), where  $I$  is the laser intensity and  $\lambda$  the laser wavelength [14, 15]. The typical temperatures are 10 - 50 keV for hot electrons and 0.1 - 5 keV for cold ones, at a laser intensity of  $10^{16}$   $\text{W}/\text{cm}^2$  [14, 15]. In this study, we propose an expansion of the two-electron-temperature plasma from the inner surface of the shell to its center. By assuming the Boltzmann distribution for hot and cold elec-

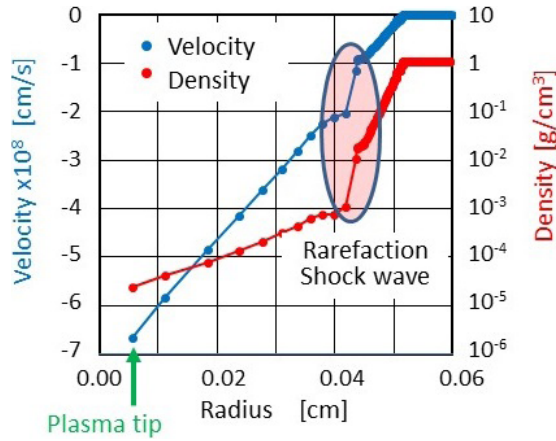


Fig. 7 Deuterium velocity and density as function of radius, when plasma reaches the shell center at 75 ps after the irradiation, for a  $D_s$  of 0.1 cm and a  $T_c$  of 1 keV.

trons and the quasi-neutrality between ions and electrons, the isothermal expansion dynamics for the plasma from the inner surface can be given as

$$-\frac{dv}{dt} = -\left(\frac{c_s}{n}\right) \frac{\partial n}{\partial r}, \quad (1)$$

where  $c_s$ ,  $t$ ,  $r$  and  $v$  are the normalized local ion sound speed  $c_s/c_{sc}$ , the normalized time  $t_c \cdot c_{sc}/R_0$ , the radius  $r/R_0$  and plasma velocity  $v/c_{sc}$ , respectively;  $R_0$  is the initial shell radius and  $c_{sc} \equiv (ZT_c/M)$  the ion sound speed determined by the cold electron temperature.

The local ion sound speed is given by

$$c_s^2 = \left(\frac{ZT_c}{M}\right) \left( \frac{1 + \frac{n_h}{n_c}}{1 + \left(\frac{T_c}{T_h}\right) \left(\frac{n_h}{n_c}\right)} \right), \quad (2)$$

where  $n$ ,  $n_h$ , and  $n_c$  are the number densities of the local ion, the hot electron, and the cold electron, respectively, and  $T_h$  is the hot electron temperature [15]. It should be noted that the ion sound speed is determined by  $T_c$ , as  $C_s^2 \approx ZT_c/M$  for  $n_c \gg n_h$  and  $c_s^2 \approx (ZT_c/M) \cdot (1 + n_h/n_c)$  for  $n_c \approx n_h$ , and it is determined by  $T_h$  as  $c_s^2 \approx ZT_h/M$  for  $n_c \ll n_h$ . Since the electrons obey the Boltzmann distribution, the local ion sound speed is determined by  $T_h$  in low density expanded regions such as  $n \ll n_0$ , where  $n_0$  is the initial shell density. Details of the model will be published elsewhere.

Figure 7 depicts the plasma expansion velocity (blue) and the normalized density  $n/n_0$  (red) as functions of the radius, just before the plasma reaches the shell center when the shell radius is 0.05 cm, the  $T_c$  1 keV, the  $T_h$  10 keV, and  $n_{h0}/n_{c0} = 1/10$ , where  $n_{c0} + n_{h0} = n_0$ . The rarefaction shock wave [16, 17] was formed near the 0.042 cm radius in the expansion of the two-electron-temperature plasma. The sound speed behind the shock wave, i.e., where  $r < 0.042$  cm, was determined by the hot electron

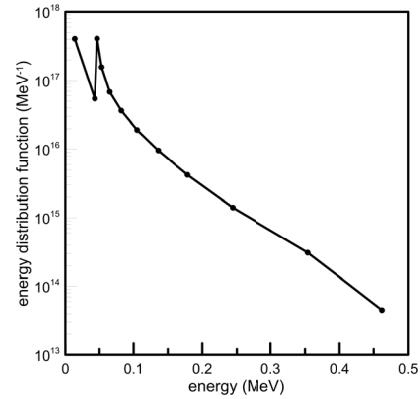


Fig. 8 Deuterium energy distribution function calculated from the plasma expansion velocity and density profiles.

temperature [16]. Then, when the plasma reaches the center at 75 ps after the irradiation, which is a shorter interval than the laser pulse duration, the expanding plasma velocity became to  $7 \times 10^8$  cm/s. This expansion velocity roughly corresponds with the observed maximum deuterium energies of 500-900 keV. With the assumption of an adiabatic expansion once the plasma tip has reached the center, the simulation also demonstrated that the hot core size was about half of the initial shell radius and the hot core lasts for over 300 ps after the laser irradiation. Both these aspects roughly agree with the observed results.

Using the plasma velocity obtained from the model given in Fig. 7, we estimated the deuterium energy distribution function, depicted in Fig. 8. We assumed that the neutrons were produced according to the following two phenomena. The red triangles (Wall) in Fig. 9 show the neutron yield for the expanded deuterium ions hitting the deuterated solid shell wall, i.e., fusion reactions between high-energy deuterium ions and cold deuterons, while the blue squares (Core) correspond to those for high-energy deuterium ions colliding each other near the shell center. For the 1 mm  $D_s$ , with  $T_h$  10 keV and  $T_c$  1 keV, the total neutron yield was  $2.8 \times 10^8$ , 70% of which was generated by the fusion reactions at the wall and the remaining 30% at the hot core. Deuterium ions of energy between 200 and 300 keV greatly contribute to the neutron generation. To estimate the neutron yield, we used empirical values of the hot and cold electron temperatures [14] from many experiments about the laser intensity at the inner surface of the spherical shell. The observed neutron yields depicted in Fig. 4 agreed fairly well with the simulated ones shown in Fig. 9.

The high neutron yield obtained with our experimental setup was due to the fact that the expansion velocity of the inner surface was mainly determined by the hot electrons. It may be possible to increase the  $T_h$  and  $T_c$  using a higher intensity laser presently available. We briefly discuss the scalability of the scheme by changing the  $T_h$  and

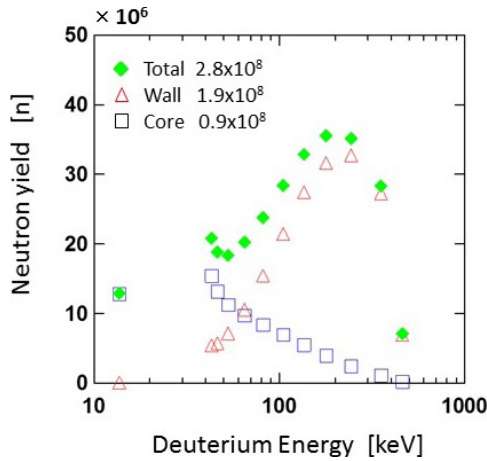


Fig. 9 Neutron yields calculated using the deuterium energy distribution function as depicted Fig. 8. The red triangles indicate neutrons generated at the shell wall by fusion reactions between high-energy deuterium ions and cold deuterons, the blue squares represent the neutron yield resulting by fusion reactions among high-energy deuterium ions near the shell center, and green squares are the sum of blue and red.

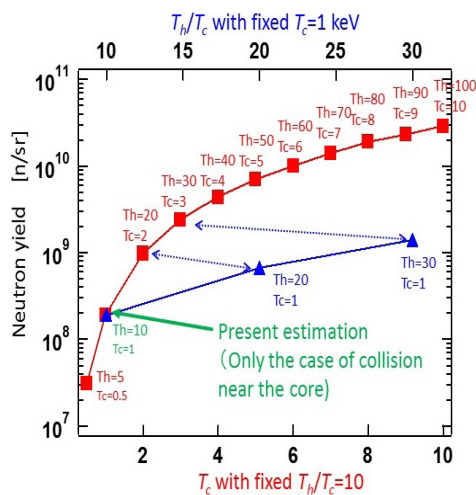


Fig. 10 Neutron yields for various temperatures ratio between hot and cold electrons. The red squares are for various  $T_c$  for the fixed temperature ratio of  $T_h/T_c = 10$ , and the blue triangles for various temperature ratio with the fixed  $T_c = 1$  keV.

$T_c$  of the model corresponding to the increase of the  $T_h$  and  $T_c$ . The red squares in Fig. 10 represent the neutron yields when increasing the cold electron temperature  $T_c$  from 0.5 to 10 keV with a fixed temperature ratio of  $T_h/T_c = 10$ , while the blue triangles indicate those obtained for larger temperature ratio and the  $T_c$  fixed at 1 keV. In both cases, a density ratio  $n_{h0}/n_{c0} = 1/10$  was assumed. The model calculation showed that  $10^{10}$  neutron yield can be achieved with a  $T_h$  above 60 keV.

## 4. Conclusion

$3 \times 10^8$  neutron generation per pulse was achieved by a GXII-HIPER irradiation through an inlet hole onto the inner surface of a spherical shell, with a laser intensity of  $(2-3) \times 10^{16}$  W/cm<sup>2</sup>. The number of neutrons generated is considerably large compared to those observed in previous experiments [13] with the same laser intensity. Despite a very simple experiment layout, the hot core formed near the shell center was surprisingly uniform, even with the one-sided laser irradiation.

We investigated the dependence of the neutron yield on the laser energy, the  $D_s$  and the  $D_h$ . Although these dependences have not been quantitatively described yet, we attempted to qualitatively explain them. For the first time, nTOF spectra were recorded at three different directions, which allowed for the demonstration of the anisotropy of the deuterium energy spectra caused by the irradiation configuration.

We have defined a simple simulation model based on a central expansion of a two-electron-temperature plasma to explain the observed neutron yields. The model calculations based on empirical values agreed well with the experimental results. The model showed that the use of a higher intensity laser would allow the generation of more than  $10^{10}$  neutrons per pulse, which is the average neutron yield required for many industrial applications. However, further investigations on this aspect need to be continued.

## Acknowledgments

The authors would like to thank GXII operation group and the plasma diagnostics operation group of the ILE, Osaka Univ. for operating these experiments, and Enago ([www.enago.jp](http://www.enago.jp)) for the English language review.

- [1] J. Alvarez *et al.*, Phys. Procedia **60**, 29 (2014).
- [2] J.A. Frenje *et al.*, Nucl. Fusion **53**, 043014 (2013).
- [3] M. Bonino *et al.*, 22nd Target Fabrication Meeting (2017).
- [4] H. Shiraga *et al.*, EPJ Web of Conferences **59**, 01008 (2013).
- [5] T. Ditmire *et al.*, Nature **398**, 489 (1999).
- [6] R. Hartke *et al.*, Nucl. Instrum. Methods Phys. Res. A **540**, 464 (2005).
- [7] F. Buerstgens *et al.*, Phys. Rev. E **74**, 016403 (2006).
- [8] T. Watari *et al.*, J. Phys.: Conference Series **688**, 012125 (2016).
- [9] M. Roth *et al.*, Phys. Rev. Lett. **110**, 044802 (2013).
- [10] H. Daido *et al.*, Appl. Phys. Lett. **51**, 2195 (1987).
- [11] N. Miyanaga *et al.*, Proceedings of 18th International Conference on Fusion Energy (2001), IAEA-CN-77.
- [12] M. Takagi *et al.*, J. Vac. Sci. Technol. Jpn. **A9**, 2145 (1991).
- [13] Y. Abe *et al.*, Appl. Phys. Lett. **111**, 233506 (2017).
- [14] K.R. Manes *et al.*, J. Opt. Soc. Am. **67**, 717 (1977).
- [15] K. Estabrook and W.L. Kruer, Phys. Rev. Lett. **40**, 42 (1978).
- [16] M. Tajiri and K. Nishihara, J. Phys. Soc. Jpn. **54**, 572 (1985).
- [17] B. Bezzerides *et al.*, Phys. Fluids **21**, 2179 (1978).